REFERENCES

[1] O. Majdani, T. S. Rau, S. Baron, H. Eilers, C. Baier, B. Heimann, *et al.*, "A robot-guided minimally invasive approach for cochlear implant surgery: preliminary results of a temporal bone study," *International journal of computer assisted radiology and surgery*, vol. 4, pp. 475-486, 2009.

[2] S. Baron, H. Eilers, B. Heimann, S. Bartling, R. Heermann, T. Lenarz, *et al.*, "Robotic-guided minimally-invasive cochleostomy: first results," *Deutsche Gesellschaft für Computer- und Roboterassistierte Chirurgie*, vol. 2, pp. 1-7, 2007.

[3] O. F. Adunka and C. A. Buchman, "Scala tympani cochleostomy I: results of a survey," *The Laryngoscope*, vol. 117, pp. 2187-2194, 2007.

[4] A. R. Lanfranco, A. E. Castellanos, J. P. Desai, and W. C. Meyers, "Robotic surgery: a current perspective," *Annals of Surgery*, vol. 239, pp. 14-21, 2004.

[5] J. E. Moore Jr and D. J. Maitland, *Biomedical Technology and Devices*: CRC press, 2013.

[6] C. Coulson, R. Taylor, A. Reid, M. Griffiths, D. Proops, and P. Brett, "An autonomous surgical robot for drilling a cochleostomy: preliminary porcine trial," *Clinical Otolaryngology*, vol. 33, pp. 343-347, 2008.

[7] L. B. Kratchman, G. S. Blachon, T. J. Withrow, R. Balachandran, R. F. Labadie, and R. J. Webster, "Design of a bone-attached parallel robot for percutaneous cochlear implantation," *IEEE Transactions on Biomedical Engineering*, vol. 58, pp. 2904-2910, 2011.

[8] T. Ota, A. Degani, D. Schwartzman, B. Zubiate, J. McGarvey, H. Choset, *et al.*, "A highly articulated robotic surgical system for minimally invasive surgery," *The Annals of thoracic surgery*, vol. 87, pp. 1253-1256, 2009.

[9] J.-J. E. Slotine and W. Li, "Applied nonlinear control," *NJ: Prantice-Hall, Englewood Cliffs*, 1991.

[10] U. Hagn, M. Nickl, S. Jörg, G. Passig, T. Bahls, A. Nothhelfer, *et al.*, "The DLR MIRO: a versatile lightweight robot for surgical applications," *Industrial Robot: An International Journal*, vol. 35, pp. 324-336, 2008.

[11]J. Huckaby and H. I. Christensen, "Dynamic Characterization of KUKA Light-Weight Robot Manipulators," Georgia Institute of Technology 2012.

[12]D. L. Peiper, "The kinematics of manipulators under computer control," Ph. D Thesis, Stanford University 1968.

[13]J. J. Craig, *Introduction to robotics: mechanics and control* vol. 3: Pearson Prentice Hall Upper Saddle River, 2005.

[14]R. P. Paul and H. Zhang, "Computationally efficient kinematics for manipulators with spherical wrists based on the homogeneous transformation representation," *The International Journal of Robotics Research*, vol. 5, pp. 32-44, 1986.

[15]J. Lloyd and V. Hayward, "Kinematics of common industrial robots," *Robotics and Autonomous Systems*, vol. 4, pp. 169-191, 1988.

[16]P. Corke, *Robotics, Vision and Control: Fundamental Algorithms in MATLAB* vol. 73: Springer Science & Business Media, 2011.

[17]B. Siciliano, L. Sciavicco, L. Villani, and G. Oriolo, *Robotics: modelling, planning and control*: Springer Science & Business Media, 2009.

[18]S. Rusinkiewicz and M. Levoy, "Efficient variants of the ICP algorithm," in *3-D Digital Imaging and Modeling, 2001. Proceedings. Third International Conference on*, 2001, pp. 145-152.

[19]B. K. Horn, "Closed-form solution of absolute orientation using unit quaternions," *Journal of the Optical Society of America. A, Optics and image science*, vol. 4, pp. 629-642, 1987.

[20]T. Yoshikawa, "Manipulability of robotic mechanisms," *The international journal of Robotics Research*, vol. 4, pp. 3-9, 1985.

[21]R. Konietschke, T. Ortmaier, H. Weiss, R. Engelke, and G. Hirzinger, "Optimal Design of a Medical Robot for Minimally Invasive Surgery, 2," *Jahrestagung der Deutschen Gesellschaft fuer Computer-und Roboterassistierte Chirurgie*, pp. 1-8, 2003.

[22]M. Mainz, *Micromotion - Micro Drive Engineering* [Online]. Available: http://micromotion-gmbh.eu/, [Accessed: 2015, May,4th].

[23]Citizen, *Citizen Micro Co. Ltd.* [Online]. Available: http://www.citizen-micro.com/pro/mortor.php, [Accessed: 2015, May, 4th].

[24]W.-Y. Lee, C.-L. Shih, and S.-T. Lee, "Force control and breakthrough detection of a bone-drilling system," *IEEE/ASME Transactions on Mechatronics*, vol. 9, pp. 20-29, 2004.

[25]J. Lee, B. A. Gozen, and O. B. Ozdoganlar, "Modeling and experimentation of bone drilling forces," *Journal of biomechanics*, vol. 45, pp. 1076-1083, 2012.

APPENDIX A. DRIVE PARAMETER IDENTIFICATION

A.1 Armature Resistance

Armature resistance was found by

1) Using a multi-meter: resistance was measured across the ports of the DC motor, the value was found to be 10.9 [Ohm]
2) With the rotor shaft fixed, a constant voltage was applied to the ports of the motor, then the current and the voltage were noted down

Table A.1: Measurements for Armature Resistance

Voltage [v]	0.62	0.72	0.84	0.94	1.06	1.17	1.29	1.39	1.51	1.59	1.73
Current [mA]	35.49	60.6	69.4	76.6	87.9	96.9	106.9	116.1	120.4	129.4	136.5

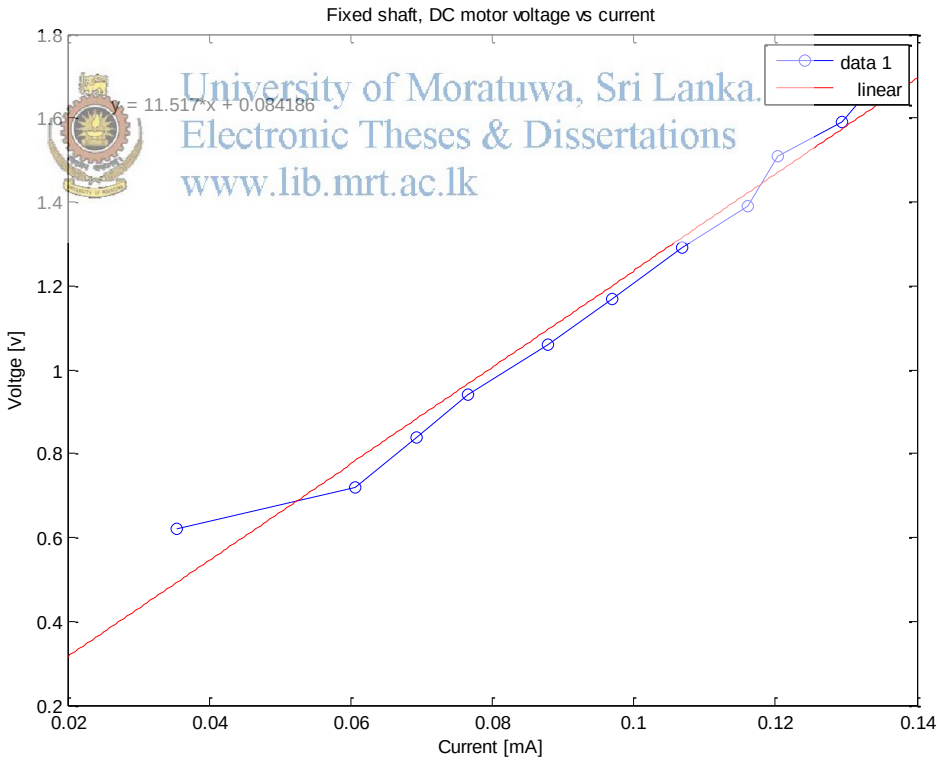

Figure A.7.1: Motor current vs. voltage

The slope gives the armature resistance, the value being 11.517 [Ohm]

A.2 **Motor Inductance**

Inductance was measured using an LCR meter. Mean value of 17 measurements were taken to be the inductance.

Table A.2: Armature Inductance Measurements

Value [uH]								
14.67	16.18	16.16	14.48	14.43	14.33	14.54	16.99	14.91
14.55	14.68	14.64	16.42	14.07	14.1	14.55	15.33	

Mean value: 15.002 [uH]

A.3 **Motor Constant**

The motor constant is equal to the induced voltage in the armature winding divided by the angular velocity

$$K_e = \frac{V_{input} - RI}{\omega(t)}$$

Where: K_e is the motor constant and $\omega(t)$ is the angular velocity.

Table A.3. Measurements for the Motor Constant

Voltage [v]	Current [mA]	Ang. Velocity [rad/s]
0.61	12.43	213.62
0.65	12.98	219.19
0.7	13.28	245.04
0.73	13.8	251.32
0.88	13.86	345.57
0.99	13.99	370.7
1.05	14.56	389.55
1.13	14.75	420.97
1.2	15.07	427.35
1.27	15.37	452.39
1.28	15.46	515.22

At different input voltages; voltage, current and angular velocity are noted down. The slope of the voltage vs. velocity gives the motor constant.

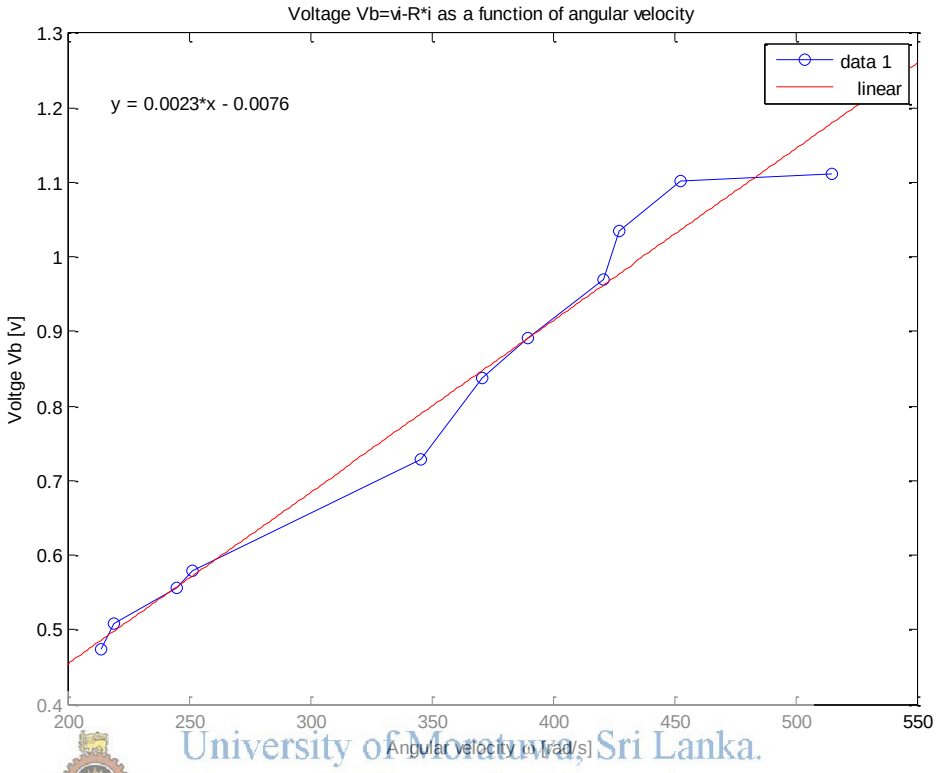

Figure A.7.2: Angular velocity vs. armature voltage

Mean motor constant: 0.0023056 [V.s]

A.4 **Motor Friction**

Motor friction is determined by measuring the armature current and angular velocity, measurements from the previous sections were used.

$$I \cdot K_t = B_m \cdot \omega_m(t) + \tau_{mdry}(t) + \tau_{mstic}(t)$$

Where: B_m is the viscous friction, τ_{mdry} is the dry friction and τ_{mstic} is the stiction of the motor. Neglecting stiction, the slope of the plot $K_t \cdot I$ vs. $\omega(t)$ gives the viscous friction of the motor. The intersection point of the y-axis gives the dry friction

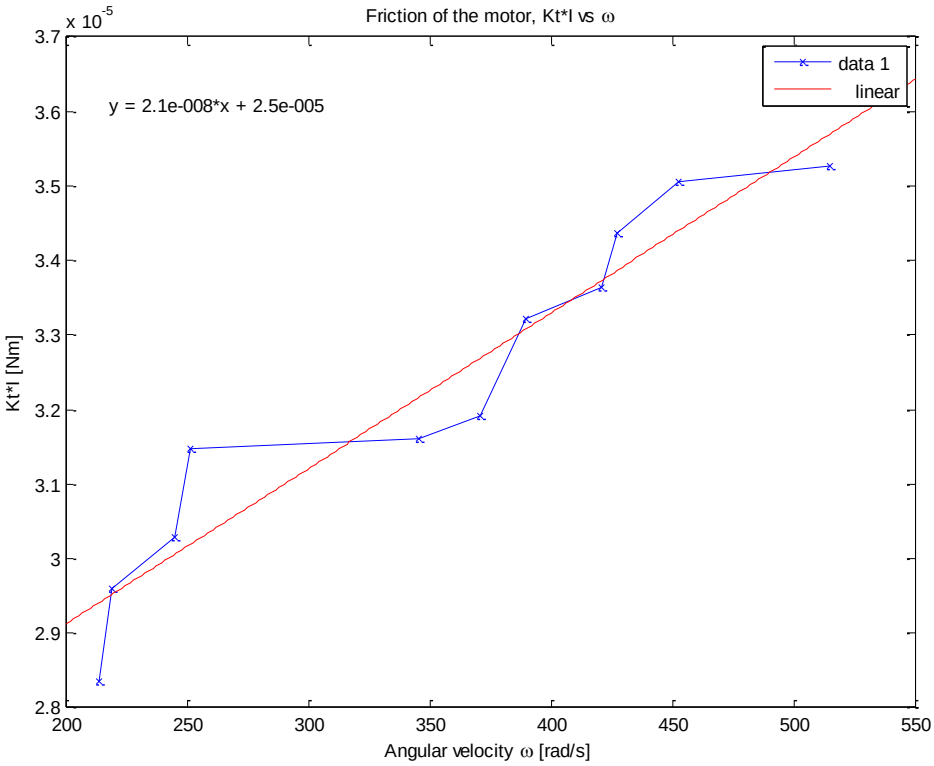

Figure A.7.3: Motor angular velocity vs. torque

The resultant viscous friction and dry friction components for the motor are:

Viscous friction: 2.0895e-008 [Nm.s]
Dry friction : 2.4939e-005 [Nm]

A.5 **Drive Friction**

Similar to motor friction, drive viscous and dry friction can be calculated via current and angular velocity measurements.

As before : $I \cdot K_t = B_m \cdot \omega_m(t) + \tau_{mdry}(t) + \tau_{mstic}(t)$

Velocity of the shaft with the gear train is estimated to be :

$$\omega_{mg}(t) = \frac{v_{input} - R \cdot I}{K_t}$$

Neglecting stiction, the slope of the plot $K_t \cdot I$ vs. $\omega(t)$ gives the viscous friction of the drive. The intersection point of the y-axis gives the dry friction

Table A.4. Measurements for the Drive Friction

Voltage [v]	Current [mA]	Ang. Velocity Gear Shaft [rad/s]	Ang. Velocity Motor shaft [rad/s]
2.44	40	4.5029	878.60
2.9	42	5.4454	1070.72
3.25	43	6.0737	1219.39
3.45	44	6.4926	1302.29
3.6	46	6.8068	1358.50
3.7	47	7.1209	1397.56

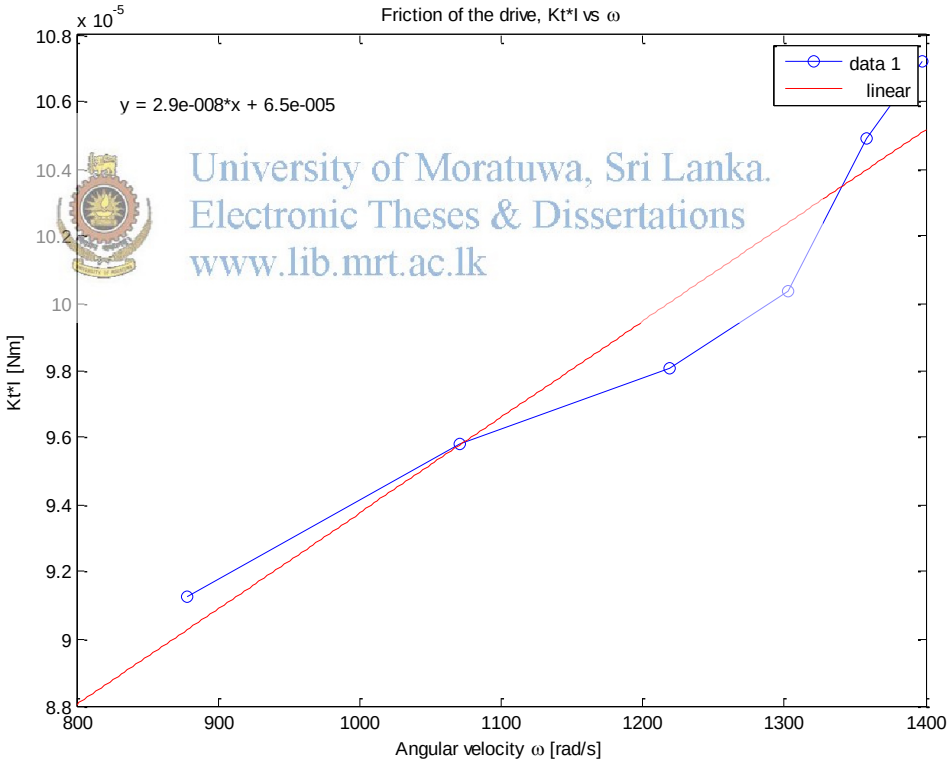

Figure A.7.4: Drive angular velocity vs. torque

The resultant viscous friction and dry friction components for the drive are:

Viscous friction: 2.8599e-008[Nm.s]
Dry friction : 6.5152e-005 [Nm]

A.6 **Motor Stiction**

Stiction torque is the starting friction imposed by the motor. By slowly increasing the torque applied to the motor shaft, it is possible to determine at what torque the motor begins to rotate. Stiction is calculated by measuring the current, at which the motor begins to rotate, and multiply by motor constant to get the torque.

The current at which the motor begins to turn : 70.5[mA];

The resultant stiction torque: 1.3586e-004 [Nm.]

A.7 **Drive Stiction**

Similar to motor stiction, starting friction of the drive, is calculated by ramping the input voltage as to increase input torque via the increasing current.

The current at which the motor begins to turn: 95.0[mA];

The resultant stiction torque: 1.9175e-004 [Nm.]

APPENDIX B. USE CASE

This section describes a simple use-case is described step-by-step. It is assumed that the Robotic manipulator and its software is setup, connected and the robotic manipulator is in the vicinity of the workspace.

1. Set to “ready pose” using the software.
2. In order to register the workspace; in the “Reg.” tab of the “Control Modes and Function; load the previously acquired model of the workspace.
3. Using “Joint/Cart.” Tabs in the Control Modes, move the manipulator to each registration point, select the corresponding registration point and its target in the “Reg.” tab. Click “Register” once the registration points are selected. Once the registration is complete. The device is ready for use.
4. In the “Path” Tab Paths can be loaded. The manipulator can traverse through a path using “Start/Stop” and “Pause” buttons

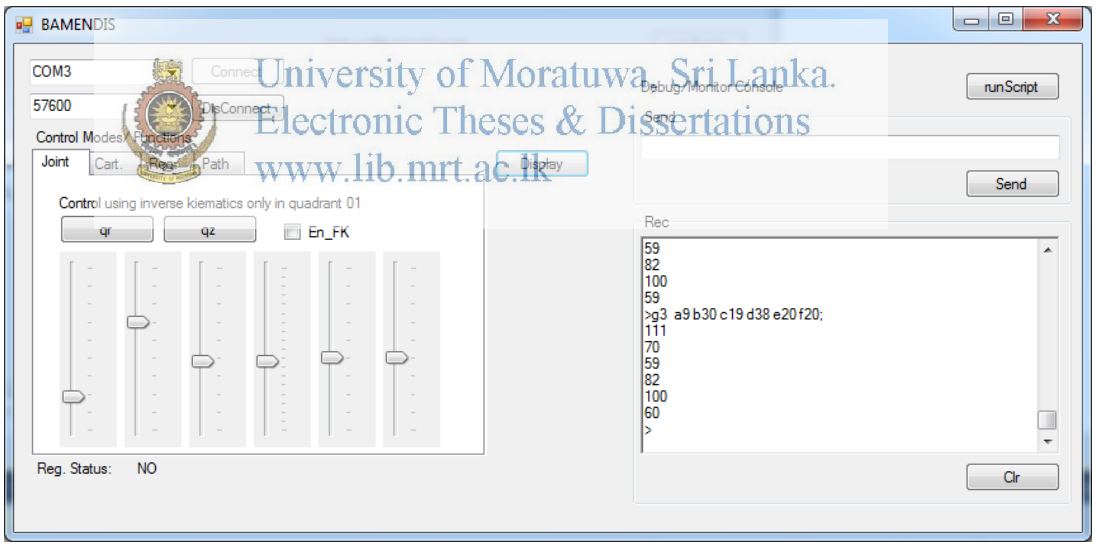

Figure A.7.5: Client software interface

APPENDIX C. LIST OF COMMANDS

C.1 Command line Syntax

G{CODE} a{value}1 **b{value}…h{value} ;**

C.2 Commands

1. Help

G0;

Command displays help message

2. Command base joints

G1 a{theta1} b{ theta2} c{theta2};

Commands the first three joints in degrees

3. Command upper joints

G2 a{theta1} b{ theta2} c{theta2};

Commands the last three joints in degrees

4. Command all joints

G3 a{theta1} b{ theta2} c{theta2} d{theta4} e{ theta5} f{theta6};

Commands the all joints in degrees

5. Command specific joint

G4 a{joint} b{ theta};

Command specific joint angle in degrees

6. Display calibration offsets

G5;

Command displays calibration offsets

7. Calibrate Write

G6 a{joint} b{value};

Writes the specific calibration value to the joint

APPENDIX D. LIST OF SIMULATION SCRIPTS

This is a list of simulation scripts, provided in the CD. The MATLAB files requires Robotic Toolbox v9.8

Model files

mdl_mbot.m	Model including tool
mdl_mbot_nt.m	Model without tool
fGenIK_c1.m	Inverse Kinematics Generator
fGenFK.m	Forward Kinematics Generator

Control Generation

My_pos_final_orig.m	Cascaded Controller, continuous, digital
disMeorig .mdl	Cascaded Controller in Simulink
disMeorigD.mdl	Cascaded Controller digital in Simulink
disMe.mdl	Position only with velocity feed forward
disMeDD.mdl	Position with velocity FF, in digital

Validators

S_hw_validation_1.m	Hardware validation of link movement
verify_IK_random	
myBot_dhMod_verif_toolbox	Verify Configuration using toolbox
myBot_dhMod_verif	Verify Manually
Dynamics.m	Calculate and verify Dynamic parameters
trajectory_algo_via_points.m	Joint space trajectory generator
ICP_validation	ICP_validation
AOQ_validation	AOQ_validation

Library generation

DoFK.m

doIK.m

GoMx.m

GoMy.m

GoMz.m

GoX.m

GoY.m

GoZ.m

probot.m mybot model, print

VB files

Vb project folder